Executive Summary

Validated Low-Speed CFD of a Blended-Wing-Body Aircraft

Kevin Armstrong II · UC Berkeley Mechanical Engineering · January 2026

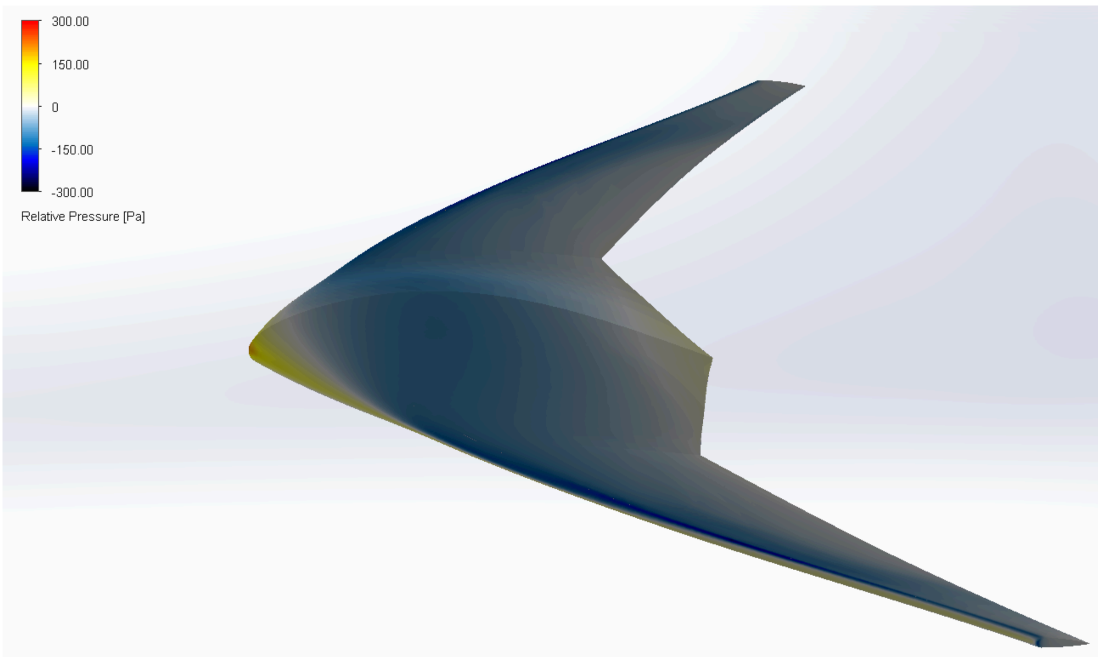

Objective

This project quantifies low-speed aerodynamics of a blended-wing-body (BWB) concept using steady-state CFD. Beyond reporting performance trends, the work establishes a repeatable analysis workflow (convergence, domain sensitivity, mesh sensitivity, consistent post-processing) suitable for early-stage concept screening. Outputs include C_L, C_D, *L/D*, and qualitative flow features from streamwise velocity cuts and surface pressure/Cp maps across an AoA sweep.

Geometry & Reference Quantities

Configuration: Swept planform BWB lifting body modeled as an external aerodynamics case.
Approximate size: Span ≈ 8 in (0.203 m), length ≈ 9 in (0.229 m), peak thickness ≈ 2 in (0.051 m).
Reference area: The aerodynamic reference area Sref was measured by sketching a top-view silhouette on the Top Plane and using SOLIDWORKS Measure. A force-to-coefficient consistency check confirms the effective Sref used by the solver:

- $S_{ref} \approx 9.62 \times 10^{-3}$ m² (≈ 14.9 in²)

From span b ≈ 0.203 m, the implied mean chord is:

- $\bar{c} \approx S_{ref} / b \approx 0.047$ m (≈ 1.86 in)

Coordinate convention: +X is freestream direction; +Z is "up." Positive AoA implemented via $V_Z > 0$, producing positive C_L.

NACA-Derived Centerbody Profile (Mid-Chord)

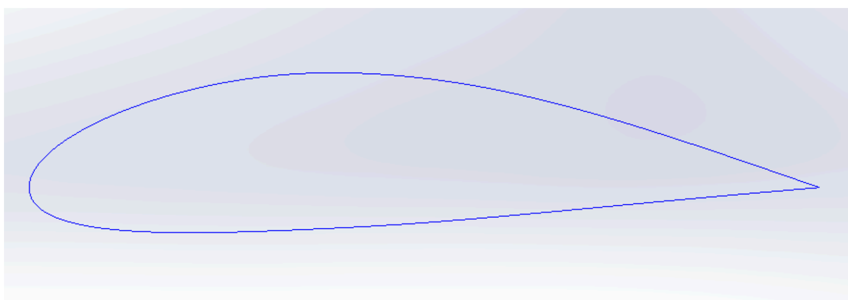

Figure ES-0. NACA-derived custom Mid-chord centerbody section used in the BWB loft

The section was generated from a NACA 00-series thickness distribution with a controlled centerbody volume term to support blending and internal packaging while maintaining a smooth leading edge and tapered trailing edge.

Freestream Conditions & Similarity Parameters

Working fluid: Air (SOLIDWORKS default).
Ambient conditions: $p_\infty = 101325$ Pa, $T_\infty = 293.2$ K.
Freestream sampling (far-field): Freestream properties were measured upstream in an undisturbed region using Point Parameters rather than surface averages.

- $\rho_\infty \approx 1.20$ kg/m³
- $\mu_\infty \approx 1.8146 \times 10^{-5}$ Pa·s
- $V_\infty \approx 40$ mph = 17.88 m/s

Dynamic pressure: $q_\infty = \frac{1}{2} \rho_\infty V_\infty^2 \approx 192$ Pa

Reynolds number (based on mean chord): $Re = \rho_\infty V_\infty \bar{c} / \mu_\infty \approx 5.6 \times 10^4$
This is a low-Reynolds-number regime, where boundary layer behavior and separation sensitivity can strongly influence drag and maximum lift.

AoA Implementation

AoA was implemented by holding geometry fixed and changing the inlet velocity direction using a 3-component velocity vector. Example for the 4° case:

- V_X = 39.9 mph, V_Y = 0 mph, V_Z = 2.79 mph
- AoA $\alpha = \arctan(V_Z / V_X) \approx \arctan(2.79/39.9) \approx 4°$

Physics Model & Boundary/Wall Inputs

- **Analysis type:** External aerodynamics, steady-state
  Flow type: Laminar and Turbulent (turbulence modeling enabled)
- **Turbulence inputs:** intensity = 1%, length scale = 0.01 m
  Walls: adiabatic, roughness = 0 µm

Convergence Protocol

Each AoA case was run until goals were marked Achieved, then continued for an additional +100 iterations to confirm stability. Reported coefficients are based on the stabilized averaged goal values after this additional iteration window.

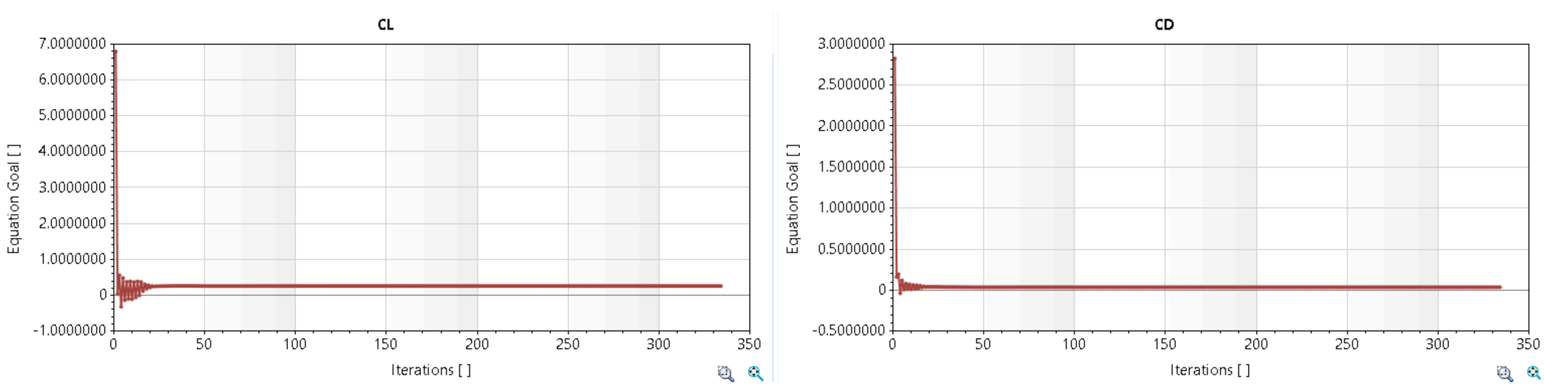

Figure ES-1. Convergence of aerodynamic goals at α = 4°. Lift and drag coefficient goals reach the solver's "Achieved" criterion and remain stable during an additional +100-iteration verification window. Final reported coefficients use the stabilized averaged values after this window to reduce sensitivity to transient iteration-to-iteration fluctuations.

Verification: Domain Independence (4° baseline, medium mesh)

Two computational domains were compared (all other settings unchanged). Coefficients show sub-1% sensitivity, supporting that far-field boundaries are not materially biasing the solution.

- **Large domain:** C_L= 0.259792, C_D= 0.0372691, *L/D* = 6.97073
- **Small domain:** C_L= 0.260230, C_D= 0.0374288, *L/D* = 6.95267

Percent differences (relative to large domain):

- $\Delta C_L \approx 0.17\%$
- $\Delta C_D \approx 0.43\%$
- $\Delta(L/D) \approx 0.26\%$

Case	CL	CD	L/D	ΔCL (%)	ΔCD (%)	Δ(L/D) (%)
Large domain	0.259792	0.037269	6.970730	+0.00	+0.00	+0.00
Small domain	0.260230	0.037429	6.952670	+0.17	+0.43	-0.26

Figure ES-2. Domain sensitivity check at α = 4° (medium mesh). Aerodynamic coefficients change by <0.5% between two domain sizes, indicating that the chosen far-field extents are sufficient for concept-level coefficient prediction under these conditions.

Verification: Mesh Independence (4° baseline, large domain)

Three mesh densities were compared. Medium → fine changes are ~1% for C_L and <0.5% for C_D, indicating near-converged coefficient values for the sweep.

- **Coarse:** C_L = 0.254886, C_D= 0.0377031, *L/D* = 6.76034
- **Medium (baseline):** C_L = 0.259792, C_D= 0.0372691,*L/D* = 6.97073
- **Fine:** C_L = 0.263079, C_D= 0.0371315,*L/D* = 7.08507

Medium → fine deltas:

- $\Delta C_L \approx 1.25\%$
- $\Delta C_D \approx 0.37\%$
- $\Delta(L/D) \approx 1.6\%$

Mesh	CL	CD	L/D
Coarse	0.254886	0.037703	6.76034
Medium (baseline)	0.259792	0.037269	6.97073
Fine	0.263079	0.037131	7.08507
Medium → Fine Δ (%)	+1.27%	-0.37%	+1.64%

Figure ES-3. Mesh sensitivity check at α = 4° (large domain). Medium ⟶ fine coefficient changes are small (≈1% for CL, <0.5% for C_D), supporting use of the medium mesh for an AoA sweep with a fine-mesh verification point.

AoA Sweep Results (−2° to +8°)

Using the validated baseline setup (large domain + medium mesh) and consistent post-processing, converged coefficients were obtained for α = −2°, 0°, 2°, 4°, 6°, 8°:

Blended Wing Body CFD Summary: Aerodynamic Coefficients vs Angle of Attack
Tabulated results (values used for plots)

AoA	CL	CD	LD
-2	-0.041385	0.028280	-1.46342
0	0.058617	0.027234	2.15237
2	0.161187	0.030716	5.24760
4	0.259792	0.037269	6.97073
6	0.355393	0.048587	7.31458
8	0.447335	0.064402	6.94595

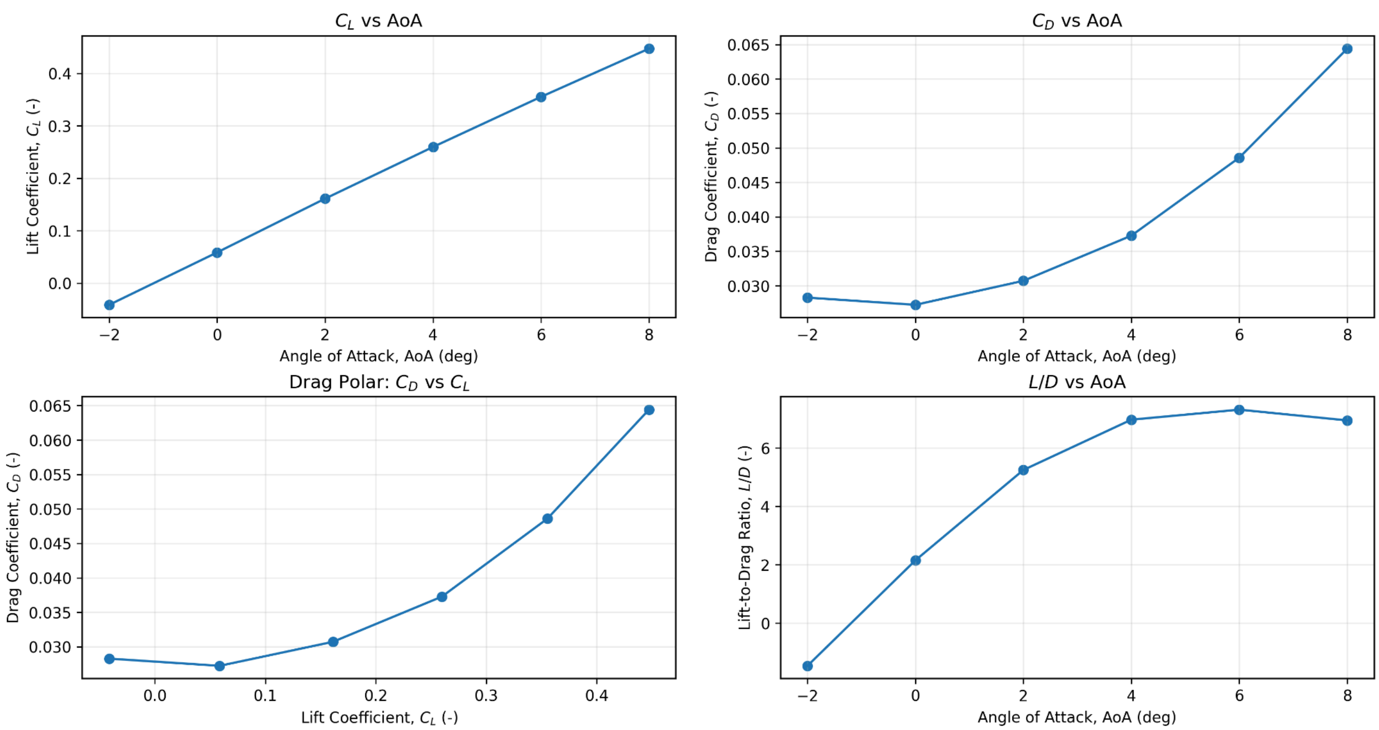

Figure ES-4. AoA sweep results for the BWB concept at V∞ ≈ 40 mph. C_L increases nearly linearly through 6°, while C_D increases with AoA after a low point near 0°. L/D peaks near 6° at ≈7.31 and declines by 8° as drag rises more rapidly.

Observed trends:

- Lift increases approximately linearly from 0° through 6°, consistent with pre-stall behavior.
- Drag is minimized near 0° and increases with AoA due to increased induced drag and growing wake losses.
- Peak aerodynamic efficiency (*L/D*) occurs near 6° in this dataset, after which*L/D* decreases as drag growth outpaces lift growth.

Flow Visualization Standard

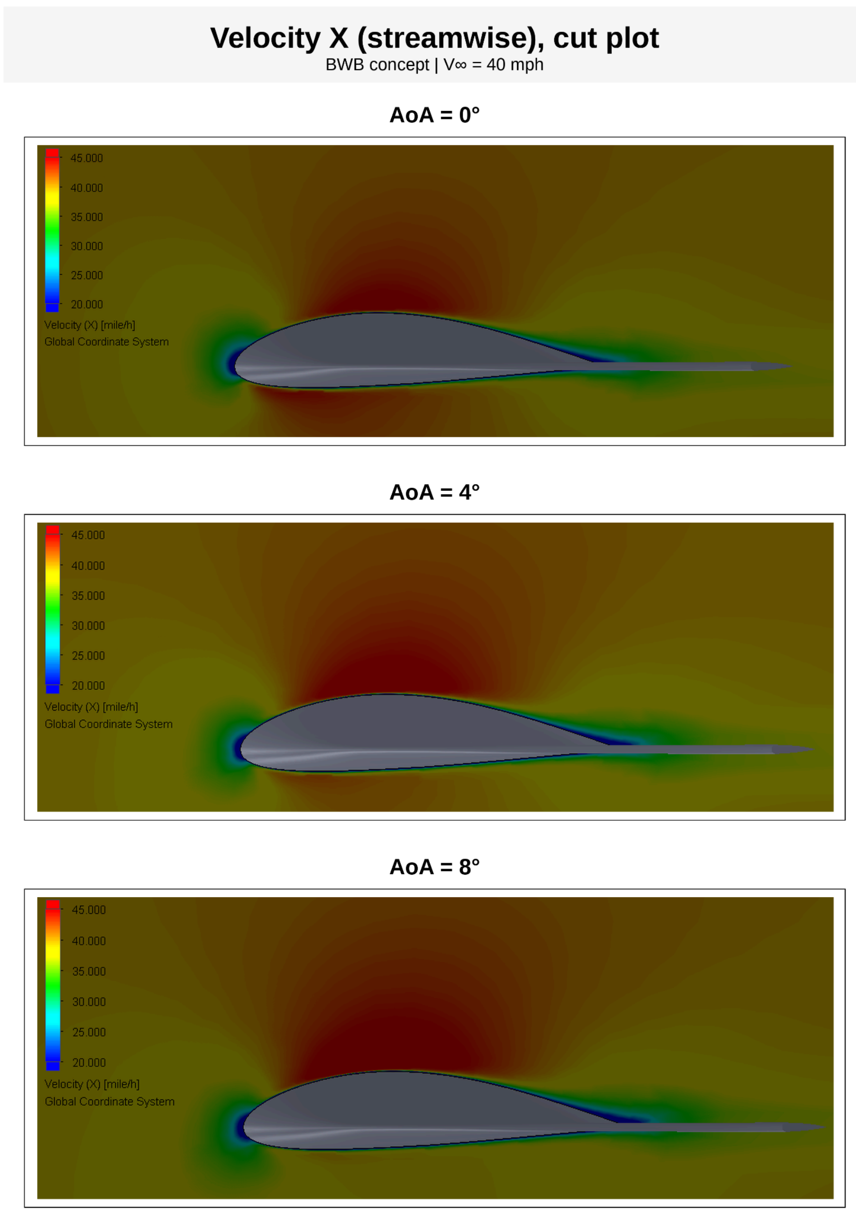

Figure ES-5. Streamwise velocity (V_x) centerline cut plots across AoA. At α = 0°, 4°, and 8° (V∞ ≈ 40 mph), the near-body acceleration region strengthens with AoA and the downstream wake thickens, indicating increased circulation and increased momentum deficit consistent with rising aerodynamic loading and drag.

For a single consistent velocity field comparison, streamwise velocity (V_X) was selected instead of velocity magnitude $|V|$. V_X most directly highlights streamwise acceleration over the body and wake momentum deficit downstream—features tied to aerodynamic loading and drag. In contrast, velocity magnitude mixes in crossflow (V_Z, V_Y) created by AoA and 3D flow, which can obscure wake-loss comparisons across AoA cases.

Pressure Coefficient Scaling

Surface maps were exported as relative static pressure, $\Delta p = p - p_\infty$, with a fixed legend scale of −300 to +300 Pa for direct comparison across cases. To relate these values to a standard aerodynamic metric, the pressure coefficient was computed using the measured freestream properties:

- $C_p = \Delta p / (\frac{1}{2} \rho_\infty V_\infty^2) = \Delta p / q_\infty$
- With $q_\infty \approx 192$ Pa, the fixed pressure legend corresponds to:
  $C_p \approx -300/192$ to $+300/192 \approx -1.56$ to $+1.56$

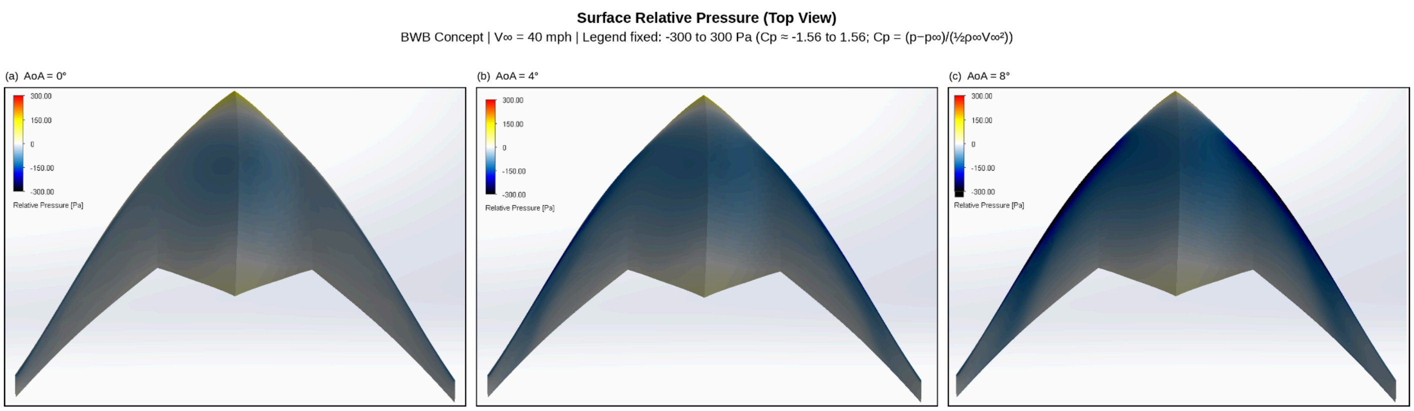

Figure ES-6. Relative static pressure, $\Delta p = p - p_\infty$, is shown for (a) $\alpha = 0°$, (b) $\alpha = 4°$, and (c) $\alpha = 8°$ at $V_\infty \approx 40$ mph using a fixed color scale (−300 to +300 Pa) to enable direct visual comparison across cases. Using freestream values sampled upstream ($\rho_\infty \approx 1.20$ kg/m³, $q_\infty \approx 192$ Pa), this legend corresponds to $C_p \approx \Delta p/q_\infty \approx -1.56$ to $+1.56$. As α increases, the suction region (negative Δp / C_p) strengthens over the forward/outer planform, consistent with the observed increase in CL in the pre-stall range.

Key Takeaways

1. Quantified aerodynamic performance: The BWB exhibits increasing lift with AoA and achieves maximum *L/D* near 6° under the tested low-speed, low-Re conditions.
2. Verification and credibility: Domain and mesh sensitivity studies show that the reported coefficients are numerically stable (sub-1% domain sensitivity; ~1% medium→fine sensitivity for C_L).

3. Consistent visualization standards: Identical camera views, fixed legends, and V_X-based slices support clean qualitative comparisons across AoA.
4. Clear nondimensional scaling: Relative pressure fields are tied to Cp using measured far-field properties, enabling standard aerodynamic interpretation.

Figure List

- **Figure ES-1:** Goal convergence history (C_L and C_D vs iteration), α = 4°
- **Figure ES-2:** Domain sensitivity check summary (large vs small)
- **Figure ES-3:** Mesh sensitivity check summary (coarse/medium/fine)
- **Figure ES-4:** AoA sweep plots + coefficient table (−2° to +8°)
- **Figure ES-5:** Velocity X (streamwise) centerline cut plots (0°, 4°, 8°)
- **Figure ES-6:** Surface relative pressure montage (0°, 4°, 8°) with Cp-equivalent scaling